Atomistic simulations for the evolution of a U-shaped dislocation in fcc Al

X. Y. Li and W. Yang
Department of Engineering Mechanics, Tsinghua University, Beijing 100084, People's Republic of China
(Received 18 May 2006; revised manuscript received 29 July 2006; published 27 October 2006)

Through massively parallel molecular dynamics simulations for the evolution of U-shaped dislocation in face-centered cubic aluminum, conventional and noncoplanar (in a helical form) evolutions of dislocation segments are revealed at the atomistic scale. The two different evolutions are closely related to the Frank-Read multiplication mechanism. The possibility of noncoplanar process is quantitatively analyzed using a combination of continuum dislocation dynamics theory and atomistic simulations. The cross-slip mechanism involving in the noncoplanar evolution is supported by examining its energy barrier and critical stress. It is suggested that the operations of two different evolutions are dictated by the strain rate and the crystal size.

DOI: 10.1103/PhysRevB.74.144108 PACS number(s): 61.72.Lk, 02.70.Ns, 62.20.Fe

I. INTRODUCTION

Plastic deformation in crystalline materials is associated with the generation, motion, and pile up of dislocations. The multiplication of dislocations is of fundamental importance in the theory of crystal deformation. The Frank-Read (FR) source[1] is a well-recognized multiplication mechanism. Such dislocation sources have been directly observed in experiments.[2,3] To investigate the evolution of FR source, Faradjian *et al.*[4] developed a continuum simulation based on dislocation dynamics. Recently, a remarkable atomistic study[5] of FR source described an anomalous multiplication process that revealed the nonlinear dislocation core effect in fcc Al. By *in situ* annealing within TEM, the modified FR mechanism[6–8] was proposed and used to explain the thermal relaxation of compositionally graded thin films.

In this paper, we show, through molecular dynamics (MD) simulations, an evolution pattern of the U-shaped dislocation in fcc Al that would enrich the FR mechanism. Direct atomistic investigation indicates that a U-shaped dislocation may behave in different manners when it emits the first dislocation loop by bowing out of an extended dislocation. One manner is that the glissile dislocation segment always bows in the original glide plane, as the conventional FR mechanism. Another is that noncoplanar composite dislocations appear owing to conservative motion of polar dislocation segments, and then bow out along each slip plane, creating a closed helical loop. The motion of these segments involves a cross-slip mechanism by which a dislocation with screw component moves from one slip plane into another.[9] Ultimately, such noncoplanar evolution results in the formation of a FR source.

As an important process, cross slip plays a significant role in the plastic deformation of metals. The studies of dislocation cross slip are considered to be challenging all along. Early theoretical approaches to study cross slip were mostly based on the line tension approximation within the framework of continuum elasticity theory. For fcc crystals, several classical models[10–12] have been proposed for cross slip occurring with the aid of thermal fluctuations. Recent advances have been attained in the field of atomistic simulations for screw dislocation cross slip. Rasmussen *et al.*[13] showed the edgelike and screwlike constrictions at the atomic-scale, and obtained the cross-slip activation energy and activation length of copper. Furthermore, the pathway, energetics,[14] and annihilation rate[15] of cross slip were investigated by Rasmussen and his co-workers. Lu *et al.*[16] estimated the dislocation constriction energy and the critical stress for cross slip via a combination of *ab initio* calculations and Peierls-Nabarro model. By performing MD simulations and experiments, Smith *et al.*[17] found that defect pile up is caused by the cross slip of dislocation loops during nanoindentation of bcc Fe single crystal. According to calculation of two-dimensional rigid dislocations, Duesbery[18] developed a cross-slip mechanism that was significantly different from the classical models. It is suggested that cross slip can occur without the constriction of the partials if the driving stress is sufficiently large.

To gain further physical insight for the competition of conventional and noncoplanar evolution mechanisms, we calculate the energy variation of dislocation configurations via a dislocation-dynamics-based continuum theory. The energy difference between two mechanisms indicated the feasibility of noncoplanar evolution at the initial stage. Because cross slip is responsible for the onset of noncoplanar evolution, the validity of cross-slip nucleation is analyzed from the critical stress and the energy barrier. Moreover, different strain rates and crystal size may lead to two evolution patterns mentioned above.

II. SIMULATION METHOD

The simulation model was constructed as a computational cell shown in Fig. 1(a). The computation cell, with a fixed height of 9.18 nm, was arranged in a perfect fcc structure. Periodic boundary conditions were enforced along the x and y directions, while the other surfaces were kept free. To minimize the effects of image forces between the dislocations and the free boundaries, a U-shaped dislocation was laid at the center of the computational cell. This U-shaped dislocation line is obtained by intercepting half of a rectangular dislocation loop, which was successfully described by de Koning *et al.*[5] The dislocation loop is achieved by placing the atoms from their fcc lattice sites in accordance with the displacement field[19] of a Volterra loop. Throughout the MD simulations, the Al embedded-atom method (EAM) potential

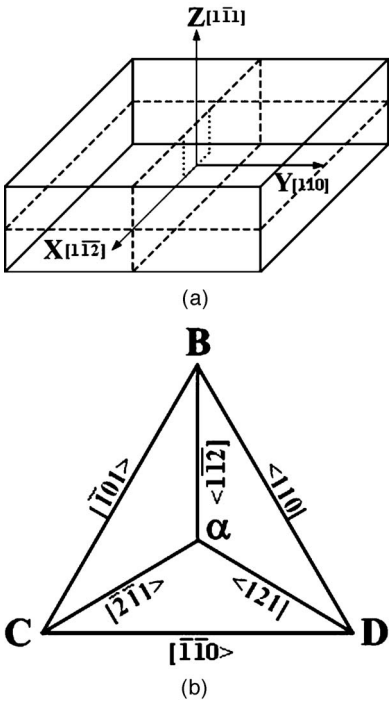

FIG. 1. (a) Schematic view of the MD computational cell. The dotted line represents half of a rectangular Volterra loop. (b) The $(\bar{1}1\bar{1})$ face of the Thompson's tetrahedron.

developed by Mishin *et al.*[20] was employed. The optimum parameters of EAM potential originate from the given database, including both experimental data and a large set of results obtained by *ab initio* calculations. The simulations were performed via a multiple time-stepping (MST) algorithm,[21] with the shorter time step being taken as 1 fs, and the longer time step 3 fs. The MST method not only speeds up simulations, but also has better convergence and stability than the conventional algorithms.

Initially, the computational system was allowed to relax for 5 ps for the sake of energy minimization. Subsequently, a simple shear strain in the y direction was imposed on the system according to a prescribed strain rate. Such shear loading was implemented by freezing the topmost $(1\bar{1}1)$ layer and fixing a constant velocity to the bottom $(1\bar{1}1)$ layer along the y direction, similarly to the procedure of literature.[22] Furthermore, the system temperature was controlled at 30 K using a Gaussian thermostat.[23] Applying such finite temperature means that the thermally activated mechanisms are likely limited, the applied shear stress becomes a significant factor in determining the deformation behaviors of metals. To identify defect types in simulated crystals, atoms in the defects were visualized by local crystalline order analysis.[24,25] Thus we define four color-mapped categories of atoms: red symbols represent atoms locating in the stacking faults, green ones represent atoms in the surface or dislocation core, yellow ones represent fully disordered atoms, and transparent ones refer to perfect atoms with local fcc order.

III. RESULTS AND DISCUSSION

During the initial free relaxation, the glissile dislocation dissociates into extended dislocations containing two Shockley partials separated by an intrinsic stacking fault. Figure 2(a) shows the initial equilibrium configuration of the U-shaped dislocation, which includes the edge dislocation dipole with Burgers vector **DC** [using Thompson notation, see Fig. 1(b)], and two partials with Burgers vectors **D**α and

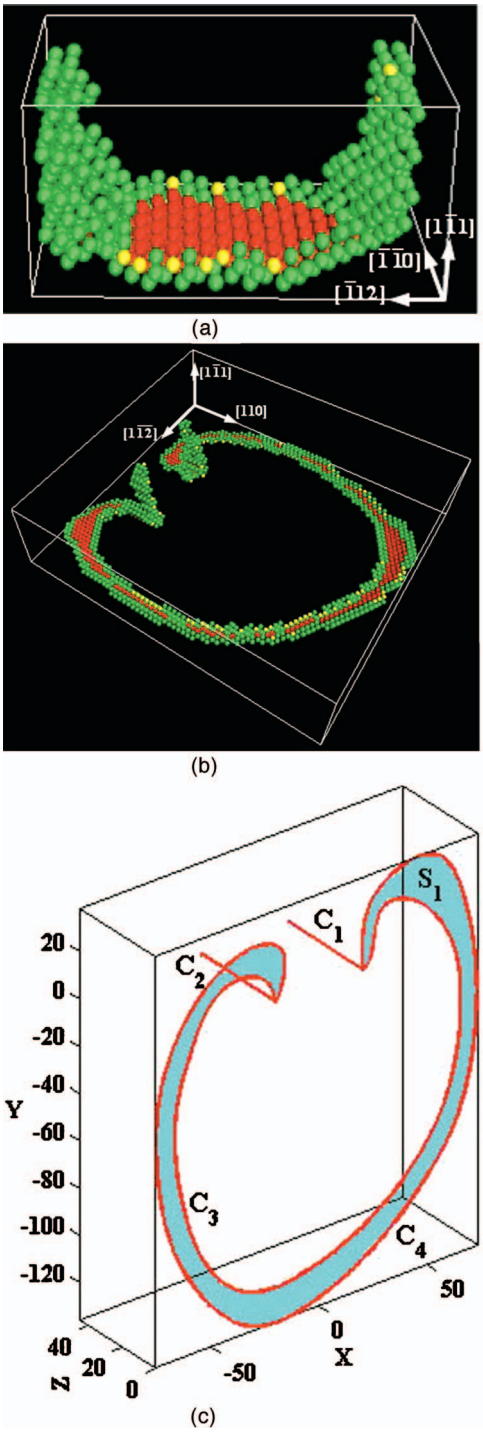

FIG. 2. (Color) (a) The equilibrium configuration of U-shaped dislocation after its thermal equilibration (zero stress). (b) Snapshot of the smaller simulated system at 10.6 ps of deformation time. (c) The continuum dislocation models corresponding to graph (b); the red curves stand for dislocation lines, and the shadow areas label stacking faults. The length unit in graph (c) is angstrom.

α**C**, respectively. Starting from this configuration, we carried out MD simulations in two computational models: one contains 391 570 atoms (with in-plane dimensions of 25.7 $\times 27.7$ nm^2) and undergoes a strain rate of 3×10^9 s^{-1}, and the other holds 6 431 614 atoms (with in-plane dimensions of 99.6×115.6 nm^2) with a strain rate of 10^9 s^{-1}. In course of simulating the smaller model, the extended dislocations bow out under the applied stress. When the stress exceeds a critical value, the bow-out of the dislocations becomes unstable. Thus the leading and trailing partials begin to bend spontaneously until they annihilate over a portion of their length. As a result, a closed extended dislocation loop forms while the U-shaped dislocation renews the original configuration. The above process repeats itself through the simulation, so that sequences of loops are emitted successively. Such multiplication mechanism is an archetype of FR source. Figure 2(b) captures a snapshot of this simulation. From this figure, we observed the asymmetric bow-out of the extended dislocation because of the variation of local line tension with the orientation.[26]

In the aforementioned simulation, the edge dislocation dipole remains immobile all along; therefore, two corners in the dislocation dipole serve as the pinning points for the glissile dislocations. At the beginning of simulation for the larger model, the glissile segments bow out and expand in the primary slip plane [Fig. 3(a)]. When the segments near two polar nodes come close to the screw orientation, the nodal glide constraints decrease so that dislocation dipole starts gliding [Fig. 3(b)]. Thus the dipoles turn into segments with screw component due to their ends terminate at the surface. Depending on the applied stress, the portion of one polar dislocation tends to cross slip onto a new slip plane, provided that it encounters an obstacle. Figures 3(c) and 3(d) describe the initial and final states of cross slip, respectively. Subsequently, the cross-slipped segment decomposes itself into partial dislocations and expands in the plane parallel to the surface. Accordingly, a noncoplanar composite dislocation forms in terms of double-coiled dislocation helix, and contains two extended dislocations and two jogs [Figs. 3(e) and 3(g)]. These extended segments sustain the shear stress, and expand on each $(1\bar{1}1)$ plane. One jog with two free ends propagates along a certain plane, whereas another jog with a fixed point keeps the mobility contributed to a gliding node. Finally, partial annihilation of the intersecting segments results in the formation of a noncoplanar composite dislocation loop as shown in Fig. 3(f). At the same time, the residual dislocation lines restore the conventional configuration of a FR source, but the dislocation dipole is shortened approximately by 4.0 nm [Fig. 3(f)]. If the shear loading is maintained on the system, the closed helical loop would continue to expand, and the residual dislocation segments would operate as a FR source.

To understand the noncoplanar evolution, it is helpful to make a quantitative calculation for the energy of the evolving system at different instants. Firstly, the dislocation lines [such as in Figs. 2(c) and 3(g)] are highlighted by fitting the positions of atoms within the dislocation cores, as made available from MD simulations. Next, the total energy and the energy density per unit length of dislocation lines are evaluated numerically. If dislocation core irregularities are neglected, the total energy of the dislocation lines is given by

$$E_{\mathrm{tot}} = \sum_{i<j} (E_{\mathrm{int}})_{ij} + \sum_i (E_{\mathrm{self}})_i + \sum_k \gamma_{\mathrm{SF}} A_k - \sum_i (W_\tau)_i, \quad (1)$$

where E_{int} represents the energy of elastic interaction between two dislocation segments, E_{self} denotes the self-energy of a dislocation segment, W_τ is the work done by the applied stress, γ_{SF} is the stacking fault energy per unit area, A_k is the area of the stacking fault marked as "S_k" in Figs. 2(c) and 3(g), and the notations i and j label the dislocation segments C_i and C_j, as shown in Figs. 2(c) and 3(g). The energy functions E_{int} and E_{self} are expressed by the well-known Blin formula,[27] and the stress work W_τ is obtained by using the increment formulae[27] as follows:

$$\delta W_\tau = \oint_C [(\boldsymbol{b}\cdot\boldsymbol{\tau})\times d\boldsymbol{l}]\cdot\delta\boldsymbol{r}, \quad (2)$$

where $\boldsymbol{b}$ is the Burgers vector, $\boldsymbol{\tau}$ is the applied stress tensor, $d\boldsymbol{l}$ is the elementary dislocation line vector, and $\delta\boldsymbol{r}$ is the displacement increment of dislocation line. Furthermore, the stacking fault energy density γ_{SF} is determined by the following expression:[28]

$$\gamma_{\mathrm{SF}} = \frac{G|\boldsymbol{b}_p|^2}{8\pi d}\left[\frac{2-\nu}{1-\nu}\left(1-\frac{2\nu\cos\theta}{2-\nu}\right)\right], \quad (3)$$

where $\boldsymbol{b}_p$ is the Burgers vector of the partial dislocation, d is the separating distance between two partials, θ is the angle of the Burgers vector with the dislocation line, and G, ν are the shear modulus and Poisson's ratio of the material. When the applied stress acts on the dislocation lines, their energy per unit length is defined as follows:

$$E_{\mathrm{per}} = \frac{\sum_{i<j}(E_{\mathrm{int}})_{ij} + \sum_i (E_{\mathrm{self}})_i}{\sum_i L_i} + \gamma_{\mathrm{SF}} d - \frac{1}{2}\sigma_E b_p d, \quad (4)$$

where L_i is the length of dislocation segment C_i, and σ_E is the Escaig stress whose component perpendicular to the total Burgers vector in the glide plane (111).[5] In Eq. (4), the first term stands for the elastic interaction energy and self-energy averaged over the entire dislocation lines, the second term describes the increment of stacking fault energy, and the last one represents the work done by the applied stress. To simplify the calculations of elastic energy per unit length, we replace it with the averaged estimate [the first term in Eq. (4)], i.e., the total elastic energy is divided by the total length of dislocations. In the practical calculation, each dislocation segment is viewed as composed of one thousand line elements. It is postulated that two elements do not interact in the proximity closer than the cutoff distance ρ, which is generally set as the core radius proportional to the length of Burgers vectors.[27] All of the parameters used in the calculation are translated from the results of MD simulations. By analyzing the linear portion of the stress-strain curves (see Fig. 5), we obtain the shear modulus of Al to be 36.43 GPa, larger than an estimate of 29.19 GPa from an analytic model (at 30 K).[29] The equilibrium splitting width d is taken as

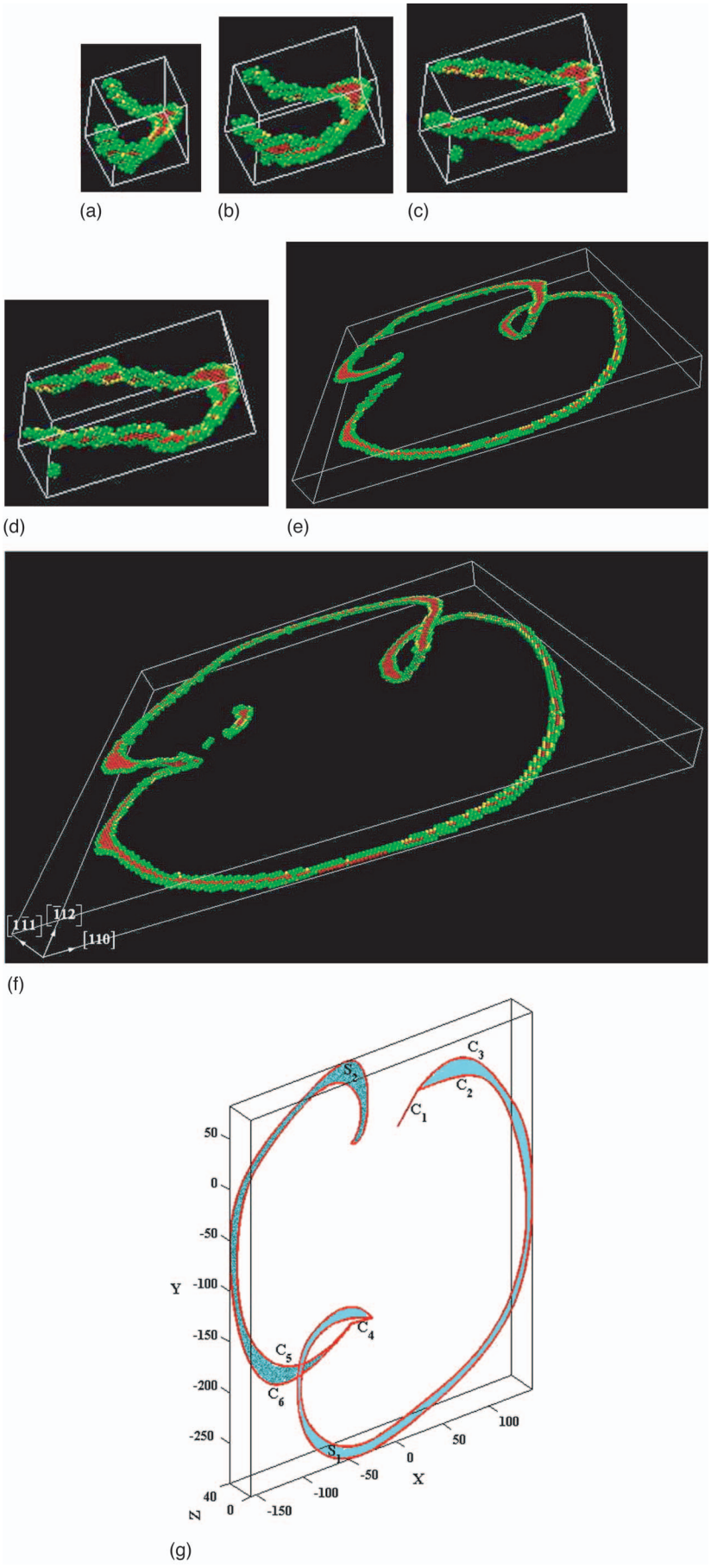

FIG. 3. (Color) (a)–(f) Snapshot of the larger simulated system at the instant of 0.2 ps, 0.6 ps, 1.0 ps, 4.0 ps, 9.8 ps, and 12.0 ps. (g) The continuum dislocation models corresponding to graph (e). The length unit in (g) is angstrom. Graphs (e) and (f) are zoomed by the half.

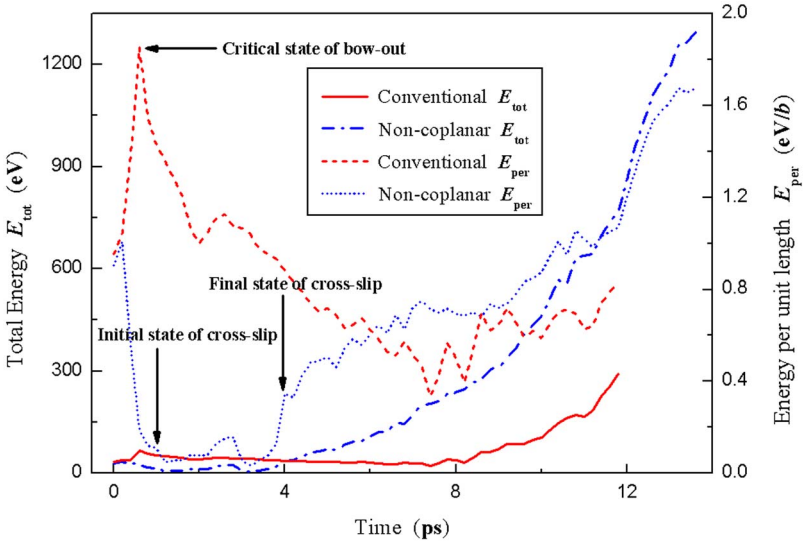

FIG. 4. (Color online) Energy vs evolution time curves during the conventional and noncoplanar evolutions.

0.93 nm by averaging the space between two partials in the MD simulations. The edge and screw components in Burgers vectors of partial dislocations are identified by lattice circuit[30] and cross-section analysis,[31] respectively.

The results of numerical calculations are plotted in Fig. 4. As illustrated by Fig. 4, the total energies of two evolutions increase with time, whereas the energy required in the noncoplanar evolution is lower than that of the conventional evolution during the initial stage. This clearly indicates that the initiation of noncoplanar evolution is energetically favorable. From the variation of energy per unit length with time, it is noted that the energy per unit length in the conventional evolution climbs steeply, and then gradually declines. On the contrary, the same energy density in the noncoplanar evolution drops rapidly and then gradually climbs. The foremost rise in the E_{per} curve of the conventional evolution implies that the glissile segment stores the energy by bending into the critical configuration. Namely, the FR source needs energy to reach the state of full activation. In Fig. 4, the peak value of E_{per} curve for conventional evolution corresponds to the activation energy of critical state. After activating the source, the E_{per} curve maintains a trend of declination, which means that the further expansion of glissile segment would be spontaneous due to the line tension. However, the glide and cross slips of dislocation dipole require less energy than the large bow-out of the glissile segment, as indicated by comparing the total energies during the two evolutions. Accordingly, the conservative motion of dislocation dipole leads to initial drop of the E_{per} curve for noncoplanar evolution. With the formation and bow-out of noncoplanar dislocations, the E_{per} curve of the noncoplanar evolution tends to ascending gradually. The initial and final times of the cross-slip process are earmarked with arrows in Fig. 4. When the cross slip takes place, the value of E_{per} is between 0.034 eV/b and 0.348 eV/b. Based on *ab initio* model calculation, the cross-slip energy barrier for Al is approximately 0.05 eV/b (Ref. 16), which just locates in the above range of E_{per}.

During the simulations, the system stress is computed by averaging the atomic stress defined through the Virial theorem.[32,33] Figure 5 demonstrates the stress-strain curves of the simulated systems, with a contrast for the applied stresses of two evolutions. The operation of the rapid bow-out of the glissile segment fixed at two nodes seems to be associated with a higher stress level, while the conservative motion of dislocation dipole requires a relatively lower stress level. Hence, the applied shear stress has a certain influence on the evolution pattern of U-shaped dislocation. For critical stress for cross slip involving thermal activation, the result from *ab initio* study is 0.32 GPa (Ref. 16) in Al. From Fig. 5, it is seen that the maximum stress required to activate cross slip is much larger than thermally activation stress. This is in fair agreement with the mechanism proposed by Duesbery.[18] The cross-slip nucleation is dominated either by thermal fluctuations or by the applied stress. The temperature of the system is maintained at 30 K during the simulation, so that the thermal fluctuation only produces low stresses which are incapable of driving cross-slip nucleation. In the absence of thermal activation, the occurrence of cross slip necessarily depends on the sufficient applied stress.

Although the applied shear stress influences the different evolutions of U-shaped dislocation, it is noted that the maximum stresses activating two evolution mechanisms are

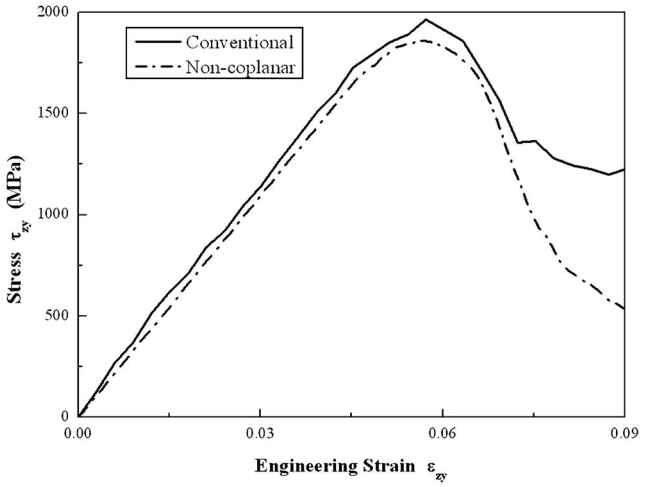

FIG. 5. Stress-strain curves during the simulations.

nearly identical. Therefore, one concludes that the strain rate and crystal size play pivotal roles in selecting the two evolutions. The high strain rate facilitates the source segment to keep a large velocity and bowed-out configuration, while the low strain rate is in favor of the conservative motion of dislocation dipole. During the simulations, the crystal boundaries are likely to provide extra resistances and constraints for the propagation of dislocation loops. Therefore the dimensional scale is thought to limit the expansion of dislocation loops. If the crystal size is larger, the dislocation loops would have wider space scale available for expanding process. The image effect for the dislocation loops also exists, when the periodic conditions are imposed on the system. This effect would result in attraction between periodic images of the expanding loops. To simplify the energy calculations, we neglect contributions of the image force in the evaluation of total energy and energy per unit length.

IV. CONCLUSIONS

To conclude, we have investigated the two evolutions of U-shaped dislocation in Al by performing MD simulations. It is found that the two evolutions furnished complementary modes for the classical FR mechanism. The energies pertinent to two evolutions are evaluated numerically via the continuum theory based on dislocation dynamics, assisted by the dislocation configurations determined by atomistic simulations. Through comparing energy difference from two evolutions, the feasibility of noncoplanar evolution leading to formation of a helical loop and then a FR source is confirmed. To elucidate noncoplanar evolution, the nucleation of cross slip is demonstrated by analyzing the energy barrier and the critical stress. In the spirit of Duesbery mechanism, cross slip can proceed regardless of the thermal activation effect, provided that the applied stress is large enough. In addition, it is found that the occurrence of a particular evolution is dictated by factors such as the strain rate and the crystal size.

ACKNOWLEDGMENTS

This research was sponsored by the 973 Project of China under Contract No. 2004CB619304, and also by the Grants No. 10332020 and No. 10121202 from the National Natural Science Foundation of China. The authors gratefully acknowledge the support of HPCS supercomputer from Chinese Academy of Meteorological Science.

[1] F. C. Frank and W. T. Read, Phys. Rev. **79**, 722 (1950).
[2] W. C. Dash, J. Appl. Phys. **27**, 1193 (1956).
[3] J. Rabier, F. Sandiumenge, J. Plain, A. Proult, and I. Stretton, Philos. Mag. Lett. **82**, 419 (2002).
[4] A. K. Faradjian, L. H. Friedman, and D. C. Chrzan, Modell. Simul. Mater. Sci. Eng. **7**, 479 (1999).
[5] M. de Koning, W. Cai, and V. V. Bulatov, Phys. Rev. Lett. **91**, 025503 (2003).
[6] F. K. LeGoues, B. S. Meyerson, and J. F. Morar, Phys. Rev. Lett. **66**, 2903 (1991).
[7] F. K. LeGoues, K. Eberl, and S. S. Iyer, Appl. Phys. Lett. **60**, 2862 (1992).
[8] F. K. LeGoues, J. A. Ott, K. Eberl, and S. S. Iyer, Appl. Phys. Lett. **61**, 174 (1992).
[9] J. S. Koehler, Phys. Rev. **86**, 52 (1952).
[10] G. Schoeck and A. Seeger, *Defects in Crystalline Solids* (Physical Society, London, 1955), p. 340.
[11] J. Friedel, in *Dislocations and Mechanical Properties of Crystals*, edited by J. C. Fisher (Wiley, New York, 1957), p. 330.
[12] B. Escaig, in *Proceedings of the Battelle Colloquium in Dislocation Dynamics*, edited by A. R. Rosenfield, G. T. Hahn, A. L. Bement, and R. I. Jaffee (McGraw-Hill, New York, 1968), p. 655.
[13] T. Rasmussen, K. W. Jacobsen, T. Leffers, and O. B. Pedersen, Phys. Rev. B **56**, 2977 (1997).
[14] T. Rasmussen, K. W. Jacobsen, T. Leffers, O. B. Pedersen, S. G. Srinivasan, and H. Jonsson, Phys. Rev. Lett. **79**, 3676 (1997).
[15] T. Vegge, T. Rasmussen, T. Leffers, O. B. Pedersen, and K. W. Jacobsen, Phys. Rev. Lett. **85**, 3866 (2000).
[16] G. Lu, V. V. Bulatov, and N. Kioussis, Phys. Rev. B **66**, 144103 (2002).
[17] R. Smith, D. Christopher, S. D. Kenny, A. Richter, and B. Wolf, Phys. Rev. B **67**, 245405 (2003).
[18] M. S. Duesbery, Modell. Simul. Mater. Sci. Eng. **6**, 35 (1998).
[19] T. A. Khraishi and H. M. Zbib, Philos. Mag. Lett. **82**, 265 (2002).
[20] Y. Mishin, D. Farkas, M. J. Mehl, and D. A. Papaconstantopoulos, Phys. Rev. B **59**, 3393 (1999).
[21] M. Tuckerman and B. J. Berne, J. Chem. Phys. **97**, 1990 (1992).
[22] M. F. Horstemeyer, M. I. Baskes, and S. J. Plimpton, Acta Mater. **49**, 4363 (2001).
[23] W. G. Hoover, *Computational Statistical Mechanics* (Elsevier, New York, 1991), p. 121.
[24] H. VanSwygenhoven, D. Farkas, and A. Caro, Phys. Rev. B **62**, 831 (2000).
[25] X. L. Ma and W. Yang, Nanotechnology **14**, 1208 (2003).
[26] G. de Wit and J. S. Koehler, Phys. Rev. **116**, 1113 (1956).
[27] J. P. Hirth and J. Lothe, *Theory of Dislocations*, 1st ed. (McGraw-Hill, New York, 1968).
[28] A. Kelly and G. W. Groves, *Crystallography and Crystal Defects* (Addison-Wesley, Reading, MA, 1974).
[29] L. Burakovsky, C. W. Greeff, and D. L. Preston, Phys. Rev. B **67**, 094107 (2003).
[30] J. Weertman and J. R. Weertman, *Elementary Dislocation Theory* (Oxford University Press, Oxford, 1992).
[31] V. Yamakov, D. Wolf, M. Salazar, S. R. Phillpot, and H. Gleiter, Acta Mater. **49**, 2713 (2001).
[32] M. P. Allen and D. J. Tildesley, *Computer Simulation of Liquids* (Oxford University Press, Oxford, 1978).
[33] J. Schiotz, T. Vegge, F. D. DiTolla, and K. W. Jacobsen, Phys. Rev. B **60**, 11971 (1999).